

SERT II: Thruster System Ground Testing

DAVID C. BYERS* and JOHN F. STAGGS†
NASA Lewis Research Center, Cleveland, Ohio

The performance of the SERT II thruster system over the range of operating parameters expected on the SERT II mission is described. Extraction voltages were varied over a range of 1000 v, and the thrust level was varied over a three to one range. At the rated (0.25-amp) beam current the over-all thruster efficiency decreased from 71% at 4770 sec specific impulse to about 68% at 4300 sec specific impulse. The required neutralizer equivalent neutral flow rate increased by about 0.007 amp when the neutralizer anode voltage was decreased from 30 to 22 v. The neutralizer flow rate more than doubled when the beam current was decreased from the rated value of 0.250 to 0.075 amp. Various life tests indicate that the operational lifetimes of all thruster components exceeded mission requirements.

Introduction

THE SERT II (Space Electric Rocket Test II) mission¹ is a 6-month life test of a 15-cm-diam, mercury, hollow-cathode thruster. The spacecraft, auxiliary space experiments, and thruster design philosophy have been described previously.^{1,2} The basic discharge-chamber optimization of the thruster for its single-design-point operation has been described in Refs. 3 and 4, which include the use of both a thermionic cathode³ and a hollow cathode.⁴ The neutralizer is of the plasma bridge type,^{5,6} and the specific configuration is based on the data presented in Ref. 7. However, several design changes have since been incorporated into the thruster, and, due to various mission constraints, it will be required to satisfy larger ranges of operating parameters than considered in previous work. A test program established its performance at lower thrust levels and determined operational procedures necessary to insure safe operation.

This paper gives details of the SERT II configuration and expected performance over the required ranges of operating parameters, including a 3:1 change in thrust level and variation of total extraction voltage by more than 1000 v. Such variations are of interest for other missions.⁸ Rather small positional variations of certain components can significantly affect performance. Data on thruster power efficiency and over-all efficiency, and some details of endurance tests are presented.

Thruster Subsystem

The SERT-II thruster subsystem is shown in Fig. 4 of a companion paper.¹ The design of the bar magnets, the accelerator and screen electrodes, the distributor pole piece, and the thruster cathode geometry was firmly established by the work presented in Refs. 3 and 4. Items that were not covered, or that required modification on the flight configuration, included the thruster propellant tank, the mercury propellant vaporizer and phase separator, the main flow orifice which divides the propellant flow between the cathode and distributor, the method of cathode keeper support, and the baffle mount.

The propellant tank has a 14.5-kg capacity and is similar to the type described in Ref. 9. It consists of a spherically shaped Hg reservoir. The rear hemisphere is formed by a butyl rubber diaphragm. Behind the diaphragm is a nitrogen

gas reservoir pressurized to 2.4×10^5 N/m² (35 psia) at the start of the mission. This pressure maintains the liquid-vapor interface at the porous tungsten disk. The Hg and nitrogen reservoirs are approximately equal in volume, so that the nitrogen pressure is reduced by half at the end of the mission.

The thruster vaporizer and phase separator (Fig. 1) is a porous tungsten plug, 0.147 cm thick, welded into a 0.635-cm-diam tubular tantalum body. The swaged heater for the vaporizer is constructed with No. 24 (0.064-cm-diam) Nichrome-V filament and Al₂O₃ insulation. A tantalum sheath is used, and commercially available cable-end seals terminate the heater. Approximately 3.5 turns of the heater are wound on the outside of the tubular vaporizer body and brazed in place. The heater is located 0.5 cm upstream of the porous tungsten disk. Contamination of the porous tungsten by various materials caused a number of problems until a rigorous fabrication procedure was established that included steps such as degreasing, ultrasonic cleaning, and vacuum firing the components at a number of points in the fabrication cycle.

In prior hollow-cathode thruster work, separate vaporizers have been used for cathode flow and main propellant flow. In present configurations, one vaporizer supplies both; a main flow orifice (Fig. 1) divides the total propellant flow between the cathode and thruster distributor. The main flow orifice is drilled in a small plug that is inserted in the downstream face of the plasma isolator (Fig. 1). Because of the lack of a reliable plasma isolator to date, the thruster systems have been fabricated with a metal mock-up of the proper

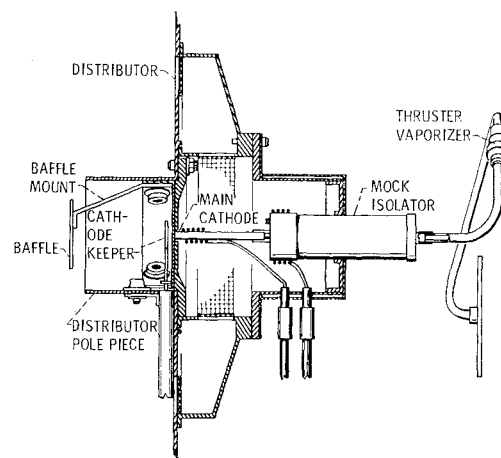


Fig. 1 Cross-sectional view of thruster propellant feed-cathode-baffle system.

Presented as Paper 69-235 at the AIAA 7th Electric Propulsion Conference, Williamsburg, Va., March 3-5, 1969; submitted March 19, 1969; revision received August 14, 1969.

* Research Scientist. Member AIAA.

† Aerospace Research Engineer; now Applications Specialist, Clevite Corporation, Cleveland, Ohio. Member AIAA.

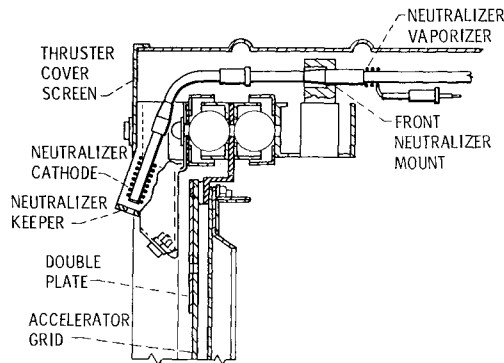


Fig. 2 Cross-sectional view of neutralizer subsystem.

dimensions. In the event that a reliable isolator becomes available, it may be substituted for the mock isolator with minimum disruption of the system integrity. The diameter of the main flow orifice is very critical to proper distribution of flows. Orifice size iterations are made until desired thruster discharge characteristics are obtained. The sizes used range from approximately 0.18 to 0.23 mm. Available drill sizes in this range increase by 0.01-mm steps starting at 0.18 mm. Orifices are drilled in the removable plugs and are then photomicrographed to determine the exact size. The orifice in the cathode is nearly constant at 0.19-mm diam.

In order to maintain the cathode keeper electrode in its position accurately, the 0.152-cm-diam tantalum keeper wire is enclosed in an Al_2O_3 tube with a tantalum sheath swaged onto the alumina and is brought into the thruster along the downstream face of the distributor. This assembly is strapped directly to the distributor. An opening at the base of the pole piece allows the keeper ring to extend into the center of the pole piece. The keeper ring is concentric with the cathode to within 0.025 cm and spaced downstream of the cathode face 0.152 ± 0.0075 cm. The positions of the legs of the three-legged baffle mount with respect to both the baffle and the distributor pole piece (Fig. 1) strongly influences thruster performance as discussed later. The tolerances on baffle position are 0.025 cm on concentricity of baffle and pole piece and ± 0.025 cm on baffle location 0.477 cm downstream of the end plane of the distributor pole piece.

Neutralizer Subsystem

The neutralizer subsystem comprises the mercury tank, vaporizer, cathode, and keeper (Fig. 2). These components are very similar to their respective counterparts on the thruster subsystem; the vaporizer and tank are basically scaled-down versions of the corresponding main thruster components. The porous tungsten plug in the neutralizer is enclosed directly in the 0.318-cm-diam feed line. The vaporizer is located ~ 10 cm along the feed line from the cathode tip. This distance eliminates thermal feedback from the cathode as a control problem but allows some heat flow to the neutralizer reservoir to assist in prevention of freezing of the Hg. The 0.469-kg-capacity tank has a butyl rubber diaphragm as in the thruster tank. A pressure transducer and thermistor will monitor its N_2 pressure and temperature on the flight system.

The neutralizer cathode fabrication is similar to that of the thruster cathode. Its orifice is ~ 0.23 mm in diameter. The position of the orifice—1.75 cm downstream of the thruster accelerator doubler plate (see Fig. 2) and 1.90 cm radially outward from the outer row of holes in the accelerator—is a critical assembly feature. The longitudinal axis of the cathode forms a 20° angle with the plane of the accelerator and is directed through the center of the exhaust beam.

The neutralizer keeper is mounted near the side of cathode and extends into position 0.152 cm downstream of the cathode face. The ring and support is fabricated of flat tantalum

sheet. Position and tolerances with respect to the cathode are the same as for the thruster main keeper-cathode assembly.

System Integration

The thruster system is mounted to a gimbal system, which in turn mounts to the spacecraft. The gimbal system consists of two rings connected by plastic bearings. The thruster system is mounted to the spacecraft by another set of bearings. The two sets of bearings allow two-dimensional thrust vectoring. The inner ring of the gimbal weighs 1.8 kg and is designed as an integral part of the thruster system. Both mercury tanks, the thruster, and cover screen that encloses the entire thruster system, are mounted from the inner ring. All of the electrical leads inside the cover screen are bare copper wires that terminate on two groupings of standoff insulators, which are shadow-shielded so as to avoid entrapment of gases and electrical breakdown.

The weight of the entire thruster system, including the thruster, mercury (15 kg), inner gimbal ring, cover screens, wiring harness, and the pressure transducer, is ~ 25 kg.

Control Logic and Power-Conditioning Outputs

An electrical schematic of the SERT II thruster system is shown in Fig. 3. The outputs of the power conditioning are of two types: controlled (or regulated) and unregulated. The unregulated outputs are approximately proportional to the output voltage of the solar cell array. The solar cell array voltage will decrease, due to radiation damage and sun-line orientation decay, by an estimated 16% over the 6-month mission lifetime.

Thruster Subsystem

Both the net accelerating potential V_I and the accelerator potential V_A are unregulated and will decrease with the solar array output voltage. For the aforementioned 16% degradation, the total accelerating voltage V_T will drop from the initial design value of 5100 v (V_I , 3000 v; V_A , 1900 v) to 4285 v, but V_I/V_T will remain approximately constant. The rate and number of high-voltage breakdowns will be monitored throughout the mission. The power supplies are adjusted so that V_I and V_A drop to zero at currents in excess of 0.300 and 0.050 amp, respectively. After an electrical breakdown the high voltage supplies recycle in 100 msec. To prevent the occurrence of sustained breakdowns, all input voltages to the thruster are automatically shut off if continuous breakdowns occur for periods in excess of 40 to 60 sec. After this type of shutdown it is necessary to restart the thruster via ground commands. The design thrust level is $\sim 2.9 \times 10^{-2}$ N (6.5 mlb), which corresponds to an ion beam current J_B of 0.25 amp at $V_A = 3300$ v. The thruster will also be required, however, to operate at about 30 and 80% of this thrust value, so that gimbal corrections may be made, if necessary, at low disturbance torques. The thrust level will be adjusted by comparing J_B with a predetermined set point and controlling J_B via a feedback loop to the thruster vaporizer. Because a single vaporizer is used, variation of the vaporizer power changes the total neutral flow through both the cathode and main flow orifices. A variation in flow, especially through the cathode,⁴ strongly alters the volt-ampere characteristic of the discharge. Thus, with this system, performance is optimized at only one set point and degrades considerably at off-design points.

The discharge potential ΔV_I may be set by ground command to provide 40, 37, or 35 v operation at about 1.8 amp discharge current. These set points are included to compensate for possible variation of the volt-ampere characteristic of the discharge plasma or drift in the power-conditioning outputs. The nominal operating point is 37 v at 1.8 amp.

The output characteristic curve of the discharge chamber supply (ΔV_I) is essentially constant voltage in the region of intersection with the discharge plasma volt-ampere characteristic curve. The no-load voltage is about 50 v in order to ensure coupling between the keeper discharge and the thruster anode. With increasing current, ΔV_I drops with approximately a $1\frac{1}{2}\text{-}\Omega$ slope. At about 2.5 amp the supply output becomes nearly current-limited, and the voltage drops to 10 v at about 2.6 amp. The current limit is included to prevent large values of discharge current which, as explained in a companion paper,¹⁰ can degrade cathode lifetime.

The cathode-tip power supply is current-limited. The cathode tip and mock isolator heater are in series. During preheat (no discharge) the heater current is set at 2.8 amp (or a cathode power of about 33 w) to heat the thruster and to insure sufficient thermionic emission for reliable ignition of the cathode keeper discharge. After the keeper discharge couples to the thruster anode, the cathode heater current drops to 1.5 amp (or a power of ~ 18 w) at a discharge current of about 0.25 amp and is constant at 1.5 amp at all higher discharge currents. The heater current is reduced to allow cooler operation of the cathode.

The thruster keeper power supply is also unregulated. The no-load supply voltage is in excess of 300 v to insure reliable starting of the keeper discharge arc. The keeper voltage V_{KK} drops with increasing keeper current from 300 v at 0.010 amp to zero at 0.300 amp. The volt-ampere characteristic curves of the keeper discharge arc and the keeper power supply intersect in the 10–15 v range, where the supply current is nearly constant. The drop in solar cell array voltage will cause a decrease in the keeper current from the initial values of 0.300 amp to about 0.270 amp over the 6-month mission.

Neutralizer Subsystem

The neutralizer tip and vaporizer heaters are in series. During preheat, previous to ignition of the neutralizer keeper discharge, the power supply current is set at 2.8 amp to insure sufficient thermionic emission and neutral flow rate for reliable ignition of the neutralizer keeper discharge. The power to the vaporizer and cathode heaters is controlled via a feedback loop which maintains a fixed voltage between the neutralizer keeper and tip.

The neutralizer keeper power supply also is unregulated. The supply voltage drops from about 300 v at 0.005 amp load to zero at about 0.200 amp. As previously stated, the keeper voltage is controlled by the neutralizer propellant flow. Two control set-points of the keeper voltage are available by ground command. Solar-cell-array degradation will cause the neutralizer keeper current to drop by $\sim 10\%$ by the end of the mission.

Thruster Subsystem Performance

Thruster parameters can be conveniently separated into those relating to the initial electromechanical configuration of the thruster and those which can be expected to vary because of degradation of the solar cell array, low-level disturbance torques, or drift in the power-conditioning outputs. The parameters of most interest are the volt-ampere characteristic of the discharge and the energy to form a beam ion, ev/ion, as a function of the propellant utilization efficiency. The former is of interest because:

- 1) The ion-chamber discharge power is the largest power loss of the thruster and hence, appreciably affects the thruster power efficiency.
- 2) The cathode lifetime is sensitive to both the voltage and current of the discharge. A companion paper¹⁰ discusses lifetime criteria in detail.
- 3) The shape of the volt-ampere curve is important in the specification of desirable power conditioning output characteristics.

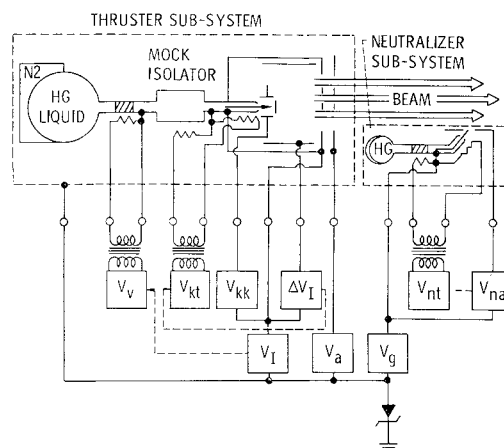


Fig. 3 Electrical schematic of SERT II thruster.

4) The discharge power strongly influences the propellant utilization efficiency. In addition, at a fixed J_B , a curve of discharge chamber losses vs propellant utilization efficiency is defined by the discharge potential.⁴

The nominal operating point of 37 v discharge potential and 1.8 amp discharge (anode) current has been selected on the basis of over-all performance and cathode lifetime. The specific electromechanical configuration has been selected to provide the nominal operating point at the midpoint of the mission.

Baffle and Baffle Mount

The baffle (Fig. 1) is identical to the 6-hole baffle described in Ref. 4. However, an additional (third) wire has been added to the baffle mount to insure adequate mechanical strength through the launch. Because the extra wire increased the discharge potential by several volts for a given ratio of cathode-to-main propellant flow, the flow ratio was increased to make the discharge characteristics identical to those of Ref. 4 (for the 6-hole baffle).

Reference 4 showed the extreme sensitivity of the thruster volt-ampere characteristic to baffle dimension and indicated that the role of the baffle was primarily electrical in nature, as opposed to an effect on neutral efflux patterns. It is not surprising, therefore, that the volt-ampere characteristics of the discharge can be very sensitive to small variations of baffle mount geometry. Due to this sensitivity, all data reported herein were taken with the final design tripod mount and 6-hole baffle system.

Ratio of Propellant Flows and Thrust Level

The thruster performance is a strong function of the neutral flow through the main and cathode orifices and the thrust level. As stated previously, the cathode/main flow ratio is controlled by diameter of the main feed orifice. The cathode orifice diameter was constant (0.19 mm) for the data presented below.

Figure 4 shows the discharge volt-ampere characteristics with three main flow orifices at three beam currents, which correspond to three required thrust levels. At $J_B = 0.25$ amp, the volt-ampere characteristics are most sensitive to a change in diameter of the main flow orifice (or ratio of cathode to main propellant flow). At lower J_B 's the volt-ampere characteristic is nearly parallel to the voltage axis and, in fact, at the lowest J_B , several prototype thrusters evidenced a negative resistance characteristic at the lower range of discharge chamber voltage. Separate tests with a two-vaporizer system (one for cathode and one for main flow) indicated that, at the rated J_B of 0.25 amp a 37-v, 1.8-amp discharge was obtained with about 0.080 equivalent amp of neutral flow through the cathode. The ratio of the cathode

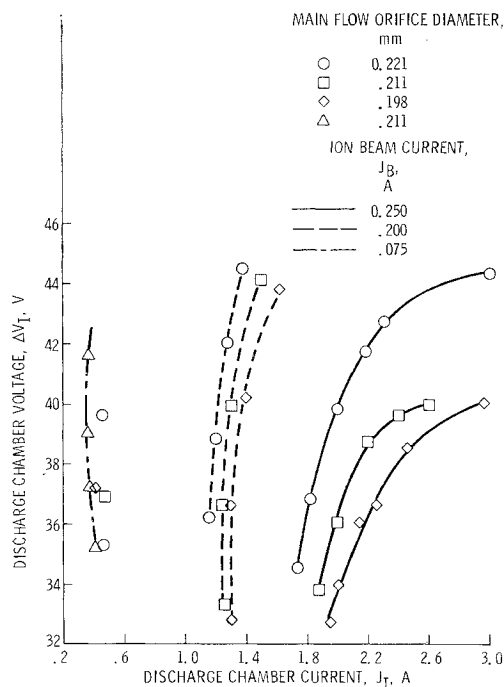


Fig. 4 Volt-ampere characteristics of SERT II thruster with three main flow orifices and at three beam currents net extraction voltage V_I , 3000 v; accelerator voltage V_A , -2000 v; cathode orifice diameter, 0.19 mm.

to main flow was about 0.37. However, the ratio of the cathode to main flow orifices is only slightly less than one. The difference in flow is explained by an effective decrease of conductance through the cathode due to the cathode discharge. The effect of the discharge on the conductance of a hollow cathode has been noted previously.¹¹ The fact that the cathode flow (0.080 amp) required to achieve the nominal discharge characteristic was larger than that required in Ref. 4 was due to the use of a 3-wire baffle mount as previously described.

Figure 5 shows the discharge current J_I vs J_B (thrust level) for 37-v discharge voltage and three main flow orifice diameters. The J_I increase is more than linear with J_B for $J_B \gtrsim$

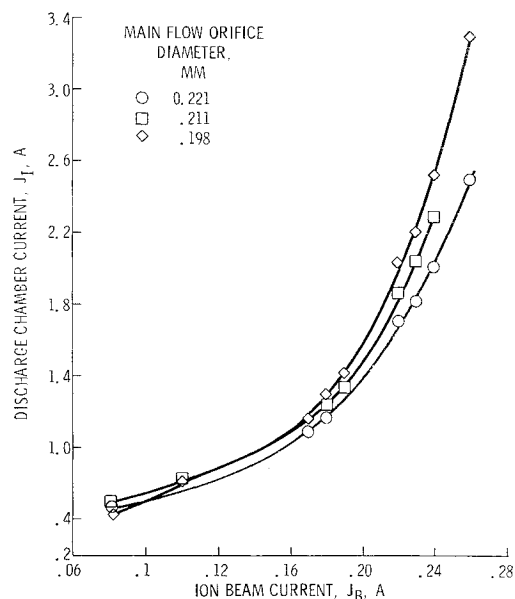


Fig. 5 Variation of discharge current with beam current. Discharge voltage ΔV_I , 37 v; net extraction voltage V_I , 3000 v; accelerator voltage V_A , -2000 v. Cathode orifice diameter, 0.19 mm.

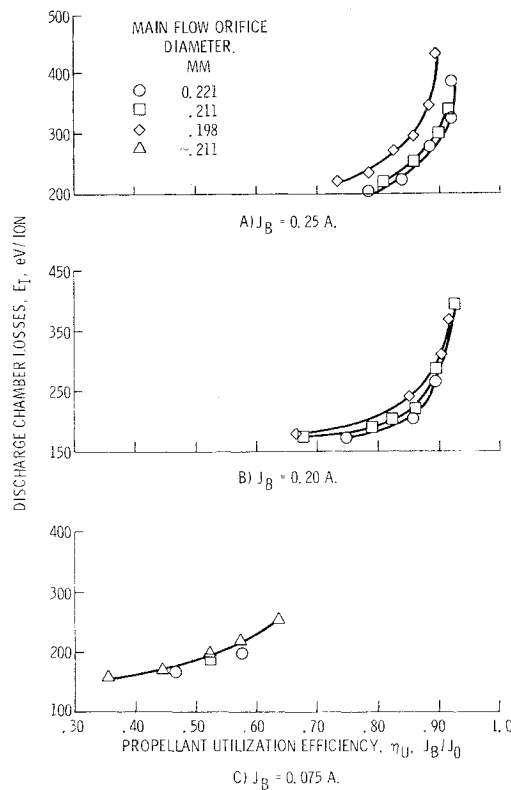


Fig. 6 Discharge chamber losses at various beam currents for various combinations of cathode and main propellant flow. Net extraction voltage V_I , 3000 v; accelerator voltage V_A , -2000 v.

0.19 amp. Then, for a fixed discharge voltage, the thruster operates at increased discharge chamber losses (eV/ion) as J_B is increased. In addition, J_I becomes more sensitive to changes in main flow orifice diameter as J_B increases. The exact reason for this behavior is not known. The ratio of flow through the cathode and main flow orifices could, however, vary more severely with increasing values of discharge current. This possibility was not investigated in these tests because the data were taken with a single vaporizer, but it is known from other tests that the discharge in the cathode strongly affects the conductance.

The energy to form a beam ion as a function of propellant utilization efficiency is shown in Fig. 6 at the three required levels of J_B . These data were generated by varying the discharge chamber voltage at fixed J_B . At $J_B = 0.25$ amp, the discharge chamber losses E_I , for a given value of propellant utilization efficiency, tend to decrease with increasing main flow orifice diameter (decreasing cathode flow). At the lower beam currents, E_I was rather insensitive to the diameter of the main flow orifice. This result is not surprising in view of the fact that the volt-ampere characteristics (or discharge chamber power) for the various orifices tended to be quite similar at the lower beam currents (Fig. 4).

Figure 7 shows propellant utilization efficiency η_U vs J_B for the three discharge voltage set-points for the SERT II mission. At a fixed discharge voltage, η_U drops as J_B drops and is comparatively insensitive to changes in main flow orifice diameter. This fact is rather surprising. As was seen in Figs. 4 and 5, the discharge currents (or discharge power losses) were, at $J_B \gtrsim 0.20$ amp, quite sensitive to the main flow orifice diameter. For example, at 0.25-amp beam current and 40-v discharge potential, E_I increased over 50% as the main flow orifice chamber decreased from 0.221 to 0.198 mm.

Figure 7 also shows that over a 2:1 range of J_B (which is of interest for larger thrusters,^{8,12}) η_U decreased by 18 to 26%. In summary, for the SERT II thruster, the propellant utilization efficiency is virtually completely specified by the dis-

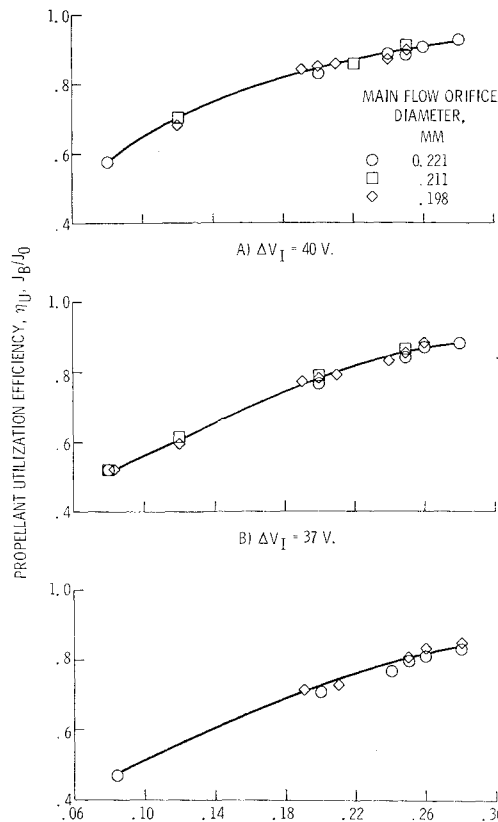


Fig. 7 Propellant utilization efficiency as a function of of beam current. Net extraction voltage V_I , 3000 v; accelerator voltage V_A , -2000 v.

charge voltage and beam current. It is not presently known whether this relationship holds for different geometries, thruster sizes, or extraction voltages.

Extraction Voltage

Figure 8 shows the effect of extraction voltage V_I on J_I , η_U , and E_I for a ratio of net to total extraction voltage of 0.62. At constant discharge potential ΔV_I and beam current, J_I decreases with increasing extraction voltage (Fig. 8a). This drop in J_I is reflected as a decrease in E_I ; however, at a fixed discharge potential, η_U remains nearly constant (Fig. 8b). Similar effects of the extraction system parameters on discharge chamber losses has been previously noted for thrusters utilizing thermionic cathodes.^{4,8,13}

Performance Variation with Mission Time

Estimates of the possible variations of several parameters during the mission because of drift in the initial set points of

Table 1 Possible deviation of parameters from design operating values and effect of deviation on discharge current

| Thruster parameter | Maximum expected deviation from design operating value | Effect of deviation on discharge current J_I |
|--------------------------------|--|--|
| Ion beam current J_B | ± 0.005 amp | +Increases J_I , -decreases J_I |
| Net extraction voltage V_I | ± 500 v | +Decreases J_I , -increases J_I |
| Cathode current J_{KT} | ± 0.1 amp | +Increases J_I , -decreases J_I |
| Discharge voltage ΔV_I | ± 1.1 v | +Increases J_I , -decreases J_I |

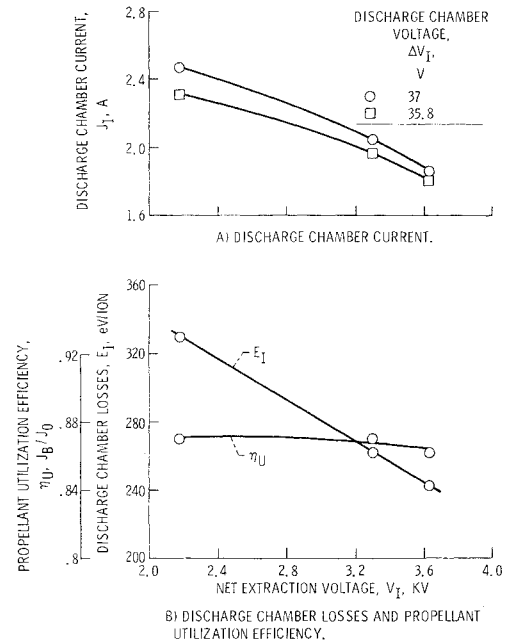


Fig. 8 Effect of extraction voltage, ion beam current J_B , 0.250 amp.

the power conditioning and loss in solar cell output are shown in Table 1. The possible variation in extraction voltage is presented as ± 500 v excursion from a nominal point. Actually during the mission the extraction voltage will decrease by about 1000 v. The other parameters shown on Table 1 can, however, either increase or decrease by the amounts shown.

The range of performance variation about an operating point is presented in Fig. 9. The variation in performance shown in Fig. 9 is representative of that possible on the SERT II mission. The solid curve is the volt-ampere characteristic taken by varying the anode voltage with all other parameters held constant. The upper and lower limits of the performed "box" are defined by the excursions of discharge voltage presented in Table 1. These excursions of discharge voltage have been estimated at about $\pm 3\%$ and are due to possible drift in the power conditioning discharge voltage set point.

The data at the right and left extremities of the performance "box" represent the sum of the deviations in the thruster electrical parameters (Table 1) which maximize or minimize the discharge current at constant discharge voltage. Figure 9 shows that a 6% variation in η_U and a 90 eV/ion variation in E_I might occur during the mission. These variations are near maximum, and it is likely that the performance will not vary this much.

Neutralizer Subsystem

The following parameters are key indicators of neutralizer performance:

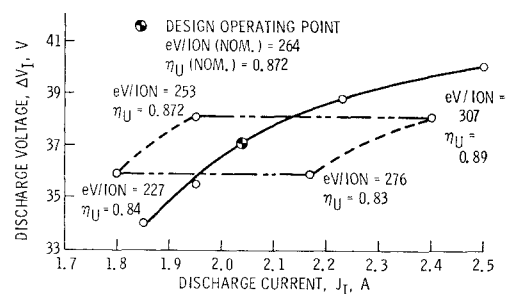


Fig. 9 Range of performance during mission.

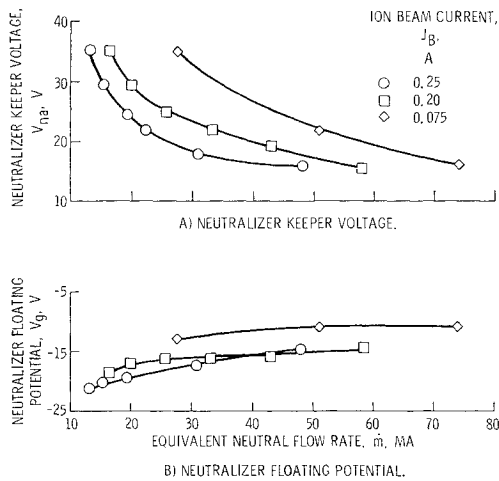


Fig. 10 Neutralizer performance as a function of flow rate and beam current.

1) The neutralizer keeper voltage with respect to the neutralizer tip, V_{na} , is controlled by the neutralizer flow rate via a feedback loop to the neutralizer vaporizer. Although use of this control logic has presented difficulties with some neutralizer geometries,¹¹ no difficulties were experienced with the SERT II geometry.

2) The beam potential V_p , downstream of the accelerator electrode varies radially and axially. Emissive probe measurements presented in Ref. 15 indicate that the potential dropped about 5 to 10 v from the axis to the beam edge. Preliminary measurements have been taken by V. K. Rawlin at NASA Lewis Research Center with a floating Langmuir probe. These results indicate that the beam potential is a strong function of both the neutralizer neutral flow rate and the symmetry of the neutralizer keeper with respect to the neutralizer cathode.

3) The neutralizer floating potential V_g (Fig. 10) is negative with respect to ground. The degree to which it floats negative decreases with neutralizer mass flow rate.

4) The coupling potential, $|V_g| + V_p$, is of importance in determining neutralizer tip lifetime, since ions may fall through this potential from the beam to the tip, causing sputtering erosion of the tip. Due to the spatial variation of V_p , however, the value of the coupling potential is somewhat arbitrarily determined.

Figure 10 shows V_{na} and V_g vs mercury flow rate at the three required ion beam currents. It is seen that the mass flow at which the neutralizer operates is a strong function of the keeper voltage. The required neutral flow rate increased by about 50% as V_{na} decreased from 30 to 22 v at each J_B . It

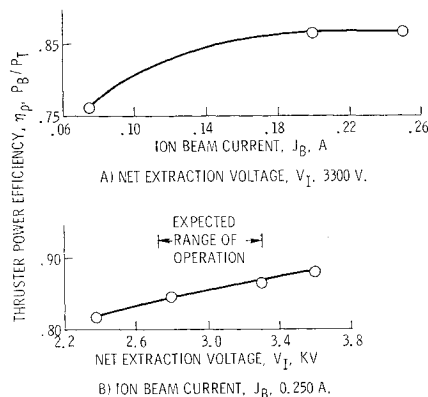


Fig. 11 Thruster power efficiency as a function of beam current and net extraction voltage. Ion chamber discharge potential ΔV_I , 37 v; ratio of net to total extraction voltage R , 0.62.

is further seen that the neutralizer performance degrades rather strongly with decreasing J_B . At fixed V_{na} 's between 30 and 22 v, the required neutral flow rate more than doubled as J_B decreased from 0.25 to 0.075 amp. Operation at reduced beam is equivalent to a radial displacement of the neutralizer away from the beam edge. Such a displacement can severely degrade performance.

Thruster Power Efficiency

Figure 11 shows the thruster power efficiency η_p vs J_B and net extraction voltage V_I . All thruster powers, including coupling power, were included in these data. Figure 11a, shows that η_p was essentially constant for $0.20 \leq J_B \leq 0.25$ amp and dropped off to ~ 0.76 at $J_B = 0.075$ amp. The near constancy in η_p at high J_B is due to the large change in J_I with thrust level (Fig. 5). The power efficiency was relatively insensitive to the extraction voltage (Fig. 11b). The ratio of net to total extraction voltage was 0.62 for the data of Fig. 11b. The extraction voltages at start of mission will be $V_I = 3300$ v and $V_a = -1980$ v. As previously mentioned, these voltages could degrade by as much as 16% over the 6-month mission; this drop will lead to a decrease in η_p of $\sim 6\%$.

Thruster Over-All Efficiency

The over-all thruster efficiency ($\eta_T = \eta_p \eta_v$) is plotted vs J_B and specific impulse (I_{sp}) in Fig. 12 for a discharge voltage of 37 v. The net extraction voltage was 3300 v for the data of Fig. 12a and varied, at $J_B = 0.25$ amp, between 3600 and 2380 v for the data of Fig. 12b. The I_{sp} was obtained by multiplying the impulse calculated from the next extraction voltage by the over-all propellant utilization efficiency (including neutralizer flow). It is seen in Fig. 12a that η_T degraded with decreasing thrust level. This reflects primarily the decrease in propellant utilization with thrust level (Fig. 7). It was seen from Fig. 5 that at fixed discharge potential the discharge chamber losses increase with thrust level. On the other hand, Fig. 7 indicated that operation at the maximum discharge voltage specified by lifetime considerations tends to maximize η_T for over-all beam currents. It should also be noted that selection of the neutralizer operating point can influence η_T (Fig. 10). Operation at 28 v neutralizer keeper voltage, compared with 22 v, decreased the neutralizer flow rate by $\sim 50\%$ and increased η_T by $\sim 2\%$.

Figure 12b shows that η_T will vary by $\sim 4\%$ due to the anticipated variations in extraction voltage over the mission time. For reference, the curve of expected future performance

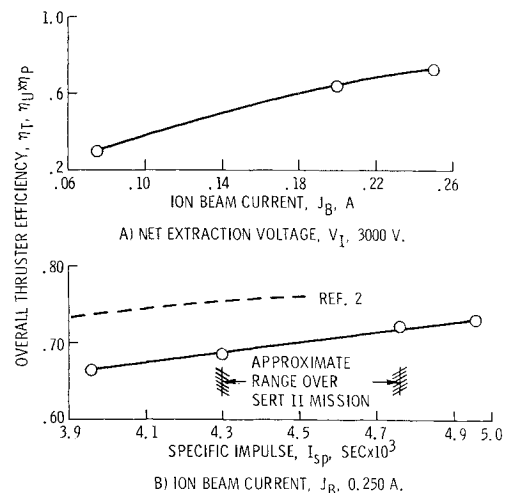


Fig. 12 Over-all thruster efficiency as a function of beam current and specific impulse. Ion chamber discharge potential ΔV_I , 37 v; ratio of net to total extraction voltage R , 0.62; neutralizer keeper voltage V_{na} , 30 v.

Table 2 Summary of life tests

| | Test | | | |
|--------------------------------|-----------------|-------------------|---------------|----------------|
| | 1 | 2 | 3 | 4 |
| Net extraction: | | | | |
| Voltage V_I , amp | 3000 | 3300 \pm 100 | 3400 | 3400 |
| Current J_B , amp | 252 | 0.250 \pm 0.005 | 0.250 | 0.250 |
| Accelerator: | | | | |
| Voltage V_A , v | 2080 | 1900 \pm 100 | 1750 | 1750 |
| Current J_A , ma | 1.2 | 2.1 | 1.52 | 1.50 |
| Discharge: | | | | |
| Voltage ΔV_I , v | 36.5 \pm 0.5 | 37.4 \pm 0.4 | 35.0 | 36 |
| Current J_I , amp | 2.01 \pm 0.02 | 1.9 \pm 0.1 | 1.9 | 1.85 |
| Thruster keeper: | | | | |
| Voltage V_{KK} , v | 10.5 \pm 0.5 | 12.0 | 11.0 | 12.3 |
| Current J_{KK} , amp | 0.34 | 0.31 | 0.34 | 0.34 |
| Neutralizer tip and vaporizer: | | | | |
| Voltage V_{NT} , v | 6.7 \pm 0.5 | 7.5 \pm 0.5 | 7.0 \pm 0.1 | 6.60 |
| Current J_{NT} , amp | 2.1 \pm 0.1 | 2.1 \pm 0.1 | 2.0 | 1.75 \pm 0.1 |
| Neutralizer anode: | | | | |
| Voltage V_{NA} , v | 22.1 | 22.0 \pm 0.5 | 29.9 | 36 |
| Current J_{NA} , amp | 0.198 | 0.215 | 0.223 | 0.22 |
| Thruster floating voltage | 11 | 20 \pm 1.0 | 20.2 | 19.0 |
| V_g , v | | | | |
| Test duration, hr | 1000 | \sim 2300 | 223 | 133 |
| Measured mass flow rates: | | | | |
| Neutralizer, ma | 18.7 | ... | ... | ... |
| Thruster, ma | 300 | ... | ... | ... |

for 2- to 3-kw thrusters utilizing SERT II technology² is also shown on Fig. 12b.

The SERT II thruster system was designed with single-point operation in mind. The variation in operating parameters produced by various mission constraints lead to degradation of thruster performance from its nominal operating point. As pointed out in Ref. 12, different designs and control logic could possibly decrease the dependence of performance on thrust level and specific impulse.

Life Tests

Four endurance tests have been performed with flight-type SERT II systems as of November 1968, three at the Lewis Research Center and one at TRW Systems Inc. (Contract No. NAS3-8917). The nominal operating parameters during the tests are presented in Table 2. Tests 1 and 2 were run at nearly similar conditions. Tests 3 and 4 differed from 1 and 2 in that the neutralizer anode control voltage was regulated at 30 and 36 v, respectively. The results of tests 1, 2, and 3 were similar in that, with the exception of the accelerator grid and cathode all thruster components had an indicated extrapolated lifetime in excess of 10,000 hr. In test 4 the neutralizer tip suffered some damage around the orifice. It is felt, then, that a neutralizer anode voltage of 30 v represents a near upper limit with the present SERT II neutralizer design.

The accelerator grid suffers from charge exchange erosion in the form of pits over the center area and a groove near the neutralizer. Erosion through the accelerator grid does not, however, indicate an end of life. As explained in a companion paper,¹⁰ electron backstreaming does not occur until holes of order 0.5 cm in radius are cut into the accelerator grid. This tolerance to large geometric variation may be due in large measure to the low beam current density near the neutralizer, where the groove erosion takes place. Measurement of the depth of charge exchange pits indicates that the minimum time for the pits to erode through the grid is in excess of 5000 hr. This estimate is probably conservative because various measurements have indicated that the rate of charge exchange erosion decreased somewhat with time. The groove erosion near the neutralizer is more severe than the pit erosion. The groove wore nearly through the grid in about 2300 hr in life test 2. Operation at increased neutralizer keeper potential

decreases the required neutral flow rate (Fig. 10). Life test 3 was operated at 30 v and measurement of the accelerator groove at 100 and 223 hr indicated that the time required to wear through is improved over that of tests 1 and 2. The "frozen" design of the SERT II thruster does not allow major mechanical changes to be made in order to improve the erosion conditions beyond mission requirements. However, in future thruster systems changes such as neutralizer position may be made to decrease erosion problems.

The discharge current started to increase, at fixed discharge voltage at about the 2200-hr point in life test 2. The increase in discharge current was felt to be due to an increase in the cathode orifice diameter. Cathode wear rates increase with increasing cathode temperature.¹⁰ To reduce the steady-state cathode operating temperature, the cathode heater and discharge currents were reduced from 2.0 amps to 1.5 and 1.8 amp, respectively. These operating conditions should result in cathode lifetimes well in excess of the mission time.

Concluding Remarks

This paper has presented performance of flight type SERT II thrusters over a wide range of operating conditions. The following results were obtained:

1) At the start of the mission the propellant utilization efficiency will be about 81.5% and the power efficiency about 86.5%. This yields an over-all efficiency of about 71% at a specific impulse of about 4770 sec. The variation of extraction voltage expected over the 6-month mission will reduce the specific impulse and over-all thruster efficiency to about 4300 sec and 68%, respectively. For these values, the beam current will remain approximately constant at 0.250 amp.

2) Thruster performance was sensitive to thrust level. A 3:1 reduction in thrust, at constant discharge voltage, decreased the propellant utilization and power efficiencies by about 35 and 8%, respectively.

3) The neutralizer performance is sensitive to thrust level and neutralizer keeper control voltage. At a fixed neutralizer keeper voltage a 3:1 reduction in thrust more than doubled the required neutralizer propellant flow. Reduction of the neutralizer keeper voltage from 30 to 22 v (the present range of interest) increased the neutral flow rate by about 50% at each of the three required thrust levels.

References

- ¹ Kerslake, W. R., Byers, D. C., and Staggs, J. F., "SERT II Experimental Thruster System," AIAA Paper 67-700, Colorado Springs, Colo., 1967; also "SERT II: Mission and Experiments," *Journal of Spacecraft and Rockets*, Vol. 7, No. 1, Jan. 1970, pp. 4-6.
- ² Kerrisk, D. J. and Kaufman, H. R., "Electric Propulsion Systems for Primary Spacecraft Propulsion," AIAA Paper 67-424, Washington, D. C., 1967.
- ³ Bechtel, R. T., "Discharge Chamber Optimization of the SERT II Thruster," *Journal of Spacecraft and Rockets*, Vol. 5, No. 7, July 1968, pp. 795-800.
- ⁴ Bechtel, R. T., Csiky, G. A., and Byers, D. C., "Performance of a 15-Centimeter Diameter, Hollow-Cathode Kaufman Thruster," AIAA Paper 68-88, New York, 1968.
- ⁵ Sohl, G., Speiser, R. C., and Wolters, J. A., "Life Testing of Electron-Bombardment Cesium Ion Engines," AIAA Paper 66-233, San Diego, Calif., 1966.
- ⁶ Sellen, J. M. and Kemp, R. F., "Research on Ion Beam Diagnostics," TRW-4381-6017-RO-000, NASA CR-54692, 1966, TRW Systems, Redondo Beach, Calif.
- ⁷ Rawlin, V. K. and Pawlik, E. V., "A Mercury Plasma-Bridge Neutralizer," *Journal of Spacecraft and Rockets*, Vol. 5, No. 7, 1968, pp. 814-820.
- ⁸ Masek, T. D. and Pawlik, E. V., "Thrust System Technology for Solar Electric Propulsion," AIAA Paper 68-541, Cleveland, Ohio, 1968.
- ⁹ Trump, G. E., "Flow Meter and Prototype Mercury Feed System Development," EOS-6969-Summary, NASA CR-54713, 1967, Electro-Optical System Inc., Pasadena Calif.
- ¹⁰ Rawlin, V. K. and Kerslake, W. R., "Durability of the SERT II Hollow Cathode and Future Applications at Higher Mission Levels," AIAA Paper 69-304, Williamsburg, Va., 1969; also "SERT II: Durability of the Hollow Cathode and Future Applications of Hollow Cathodes," *Journal of Spacecraft and Rockets*, Vol. 7, No. 1, Jan. 1970, pp. 14-20.
- ¹¹ Kemp, R. F. and Hall, D. F., "Ion Beam Diagnostics and Neutralization," TRW-06188-6011-R000, NASA CR-72343, 1967, TRW Systems, Redondo Beach, Calif.
- ¹² Bechtel, R. T., "Performance and Control of a 30-Centimeter Diameter Low Impulse Kaufman Thruster," AIAA Paper 69-238, Williamsburg, Va., 1969; also *Journal of Spacecraft and Rockets*, Vol. 7, No. 1, Jan. 1970, pp. 21-25.
- ¹³ Byers, D. C., "An Experimental Investigation of a High-Voltage Electron-Bombardment Ion Thruster," *Journal of the Electrochemical Society*, Vol. 116, No. 1, Jan. 1969, pp. 9-17.
- ¹⁴ Reader, P. D., "Investigation of a 10-Centimeter-Diameter Electron-Bombardment Ion Rocket," TN D-1163, 1962, NASA.
- ¹⁵ Ward, J. W. and King, H. J., "Mercury Hollow Cathode Plasma Neutralizers," *Journal of Spacecraft and Rockets*, Vol. 5, No. 10, Oct. 1968, pp. 1161-1164.

JANUARY 1970

J. SPACECRAFT

VOL. 7, NO. 1

SERT II: Durability of the Hollow Cathode and Future Applications of Hollow Cathodes

VINCENT K. RAWLIN* AND WILLIAM R. KERSLAKE†
NASA Lewis Research Center, Cleveland, Ohio

The SERT II thruster uses mercury-vapor-fed hollow cathodes for both the main discharge chamber and for the neutralizer cathode. The design of these two nearly identical cathodes was determined by a previous development program. This paper presents the results of life testing seven main cathodes and six neutralizer cathodes in experimental thruster systems for periods up to 3438 hr. The main cathode emits 2 amp to the discharge chamber and has at this current, a maximum projected lifetime of 15,000 hr. When emission currents greater than 2.5 amp were drawn, the projected lifetime was sharply reduced. The neutralizer cathode injects 0.25 amp of electrons into the ion exhaust beam and has a maximum projected lifetime of 33,000 hr. A hollow cathode has been tested in a bell jar as a simulated neutralizer for more than 12,000 hr. Larger hollow cathodes developed for use in large thrusters emitted 10 to 20 amp and showed no wear after testing for 234 hr.

Introduction

A 15-CM-DIAM Kaufman thruster, using Hg propellant, will be used on the SERT II (Space Electric Rocket Test II) mission.¹ A development program was carried out at the NASA Lewis Research Center which specified the optimum experimental thruster components.²⁻⁴ A part of that program consisted of endurance testing the final experimental thruster design for more than 2000 hr.

The experimental thruster was similar to the thruster system described in Ref. 5. The major difference was that the mercury vapor flow was not split between the cathode and discharge chamber. Instead two vaporizers were used—

one for the hollow cathode and the other for the main discharge chamber. The experimental thruster also had the advantage of being easily modified for improvements or parts replacement.

This paper presents the endurance test results for the main discharge cathode and neutralizer cathode used in that program. Also discussed are two areas of concern relating to the plasma-bridge neutralizer. The paper also presents the results obtained with the SERT II and larger hollow cathodes when operated at higher emission currents.

Experimental Apparatus

A cross section sketch of the hollow cathode used for the SERT II experimental neutralizer and main thruster cathode is presented in Fig. 1 and is further described in Ref. 2. The main thruster cathodes and the neutralizer cathodes were

Presented as Paper 69-304 at the AIAA 7th Electric Propulsion Conference, Williamsburg, Va., March 3-5, 1969; submitted October 30, 1968; revision received August 14, 1969.

* Aerospace Research Engineer.

† Head, Propulsion Systems Section. Member AIAA.